

# Treatment of Canine Oral Melanoma with Nanotechnology-Based Immunotherapy and Radiation

P. Jack Hoopes,<sup>†,§,||</sup> Robert J. Wagner,<sup>†</sup> Kayla Duval,<sup>§</sup> Kevin Kang,<sup>§</sup> David J. Gladstone,<sup>†,§,||</sup> Karen L. Moodie,<sup>†</sup> Margaret Crary-Burney,<sup>†</sup> Hugo Ariaspulido,<sup>†</sup> Frank A. Veliz,<sup>‡</sup> Nicole F. Steinmetz,<sup>‡,\*</sup> and Steven N. Fiering<sup>†,\*</sup>

<sup>†</sup>Geisel School of Medicine at Dartmouth, Hanover, New Hampshire 03755, United States

<sup>‡</sup>Case Western Reserve University, Cleveland, Ohio 44106, United States

<sup>§</sup>Thayer School of Engineering at Dartmouth, Hanover, New Hampshire 03755, United States

<sup>||</sup>Section of Radiation Oncology, Dartmouth Hitchcock Medical Center, Lebanon, New Hampshire 03766, United States

**ABSTRACT:** The presence and benefit of a radiation therapy-associated immune reaction is of great interest as the overall interest in cancer immunotherapy expands. The pathological assessment of irradiated tumors rarely demonstrates consistent immune or inflammatory response. More recent information, primarily associated with the “abscopal effect”, suggests a subtle radiation-based systemic immune response may be more common and have more therapeutic potential than previously believed. However, to be of consistent value, the immune stimulatory potential of radiation therapy (RT) will clearly need to be supported by combination with other immunotherapy efforts. In this study, using a spontaneous canine oral melanoma model, we have assessed the efficacy and tumor immunopathology of two nanotechnology-based immune adjuvants combined with RT. The immune adjuvants were administered intratumorally, in an approach termed “in situ vaccination”, that puts immunostimulatory reagents into a recognized tumor and utilizes the endogenous antigens in the tumor as the antigens in the antigen/adjuvant combination that constitutes a vaccine. The radiation treatment consisted of a local 6 × 6 Gy tumor regimen given over a 12 day period. The immune adjuvants were a plant-based virus-like nanoparticle (VLP) and a 110 nm diameter magnetic iron oxide nanoparticle (mNPH) that was activated with an alternating magnetic field (AMF) to produce moderate heat (43 °C/60 min). The RT was used alone or combined with one or both adjuvants. The VLP (4 × 200 μg) and mNPH (2 × 7.5 mg/gram tumor) were delivered intratumorally respectively during the RT regimen. All patients received a diagnostic biopsy and CT-based 3-D radiation treatment plan prior to initiating therapy. Patients were assessed clinically 14–21 days post-treatment, monthly for 3 months following treatment, and bimonthly, thereafter. Immunohistopathologic assessment of the tumors was performed before and 14–21 days following treatment. Results suggest that addition of VLPs and/or mNPH to a hypofractionated radiation regimen increases the immune cell infiltration in the tumor, extends the tumor control interval, and has important systemic therapeutic potential.

**KEYWORDS:** magnetic nanoparticle, hyperthermia, immunotherapy, virus-like nanoparticle (VLP), in situ vaccination, radiation therapy, abscopal effect

## INTRODUCTION

Immunotherapy to treat cancer is being aggressively developed and clinically utilized. With respect to immunotherapy and radiation treatment, new research studies are beginning to confirm what has long been theorized, that local radiation treatment has a very important immune component that can be enhanced by appropriate RT dose delivery and the addition of compatible immune stimulants.<sup>1–3</sup> In previous studies, we have shown that moderate magnetic nanoparticle hyperthermia (mNPH) treatment of an established murine melanoma tumor can generate immune-based systemic resistance to tumor rechallenge in a contralateral tumor in the same mouse.<sup>4</sup>

Radiation is a well-established local cancer therapy that rarely demonstrates the ability to affect unirradiated metastatic tumors distant from the primary tumor treatment site. This uncommon and unpredictable effect on untreated tumors is termed the “abscopal effect”, and while it is accepted to be immune-based, the pathophysiologic mechanisms are not well-defined.<sup>2</sup> This immune basis of the abscopal effect got initial support from

mouse studies performed more than 39 years ago demonstrating the contribution of T cells to radiation-induced tumor control.<sup>5</sup> Recent clinical studies have begun to show that radiation and immunotherapy treatments such as checkpoint inhibitors are capable of generating a quantifiable positive response in unirradiated tumors.<sup>6–8</sup> Another recent radiation-abscopal effect study of more than 6000 men with metastatic prostate carcinoma, treated with local prostate RT + androgen deprivation therapy, demonstrated significant improvement in the overall survival rate, as compared to androgen deprivation therapy alone.<sup>9</sup> This study shows that the treatment of a primary prostate tumor with RT can improve the outcome for

**Special Issue:** New Directions for Drug Delivery in Cancer Therapy

**Received:** February 5, 2018

**Revised:** March 24, 2018

**Accepted:** April 3, 2018

**Published:** April 3, 2018

patients with metastatic disease. Other important factors when assessing the immune effects of RT are radiation fraction number and size. Recent studies indicate that a single radiation dose compared to multiple smaller radiation doses, at the same effective total dose, induces markedly different gene and protein expression profiles.<sup>10,11</sup> Many believe that delivering RT with larger but fewer doses/fractions (hypofractionated RT, HFRT), while potentially more damaging to normal tissue, might be more immunogenic and therapeutically effective.<sup>12–14</sup> The basic concept of the impact of RT on the antitumor immune response is that RT damages the tumor and/or microenvironment to create a more immunogenic local environment.<sup>15</sup>

RT by itself is rarely sufficient to create clinically effective antitumor immunity.<sup>16,17</sup> Rather, the common local response to RT is thought to be immunosuppressive. Studies suggest that RT damage generally recruits M2-type tissue repair macrophages that suppress adaptive immunity.<sup>18</sup> The crucial aspect appears to be the potential of RT to generate an “immunogenic cell death” (ICD) or sublethal injury that occurs when cells die or are altered in a manner that stimulates an immune response.<sup>19</sup> ICD is characterized by a grouping of danger-associated molecular signals (DAMPs), among which are calreticulin expression on the cell surface, release of ATP, release of HMGB1 protein, and expression of type one interferons.<sup>2</sup> When the tumor environment is sufficiently immunogenic, tumor-associated antigens and neoantigens are taken up by antigen presenting cells that go to the lymph nodes, present these antigens to T cells, and stimulate an adaptive immune response against tumor cells. This adaptive immune response not only impacts local tumors but can also generate a systemic response against the same tumor in unirradiated sites.<sup>4</sup> Recent studies using T-cell receptor (TCR) transgenic mice have shown that radiation can prime T cells to interact with exogenous tumor antigens<sup>4,20</sup> and that radiation can induce a tumor specific T cell response and subsequent immunogenic cell death.<sup>21</sup>

In vivo murine tumor studies have demonstrated the safety, efficacy, and abscopal-type effects<sup>22–24</sup> of both mNPH<sup>25,26</sup> and VLP.<sup>27,28</sup> Additional studies have demonstrated the improved tumor treatment efficacy when combining mNPH with radiation.<sup>29</sup> We have used this information to assess the feasibility and efficacy of two different nanotechnology-based immune adjuvants (mNPH and VLP) combined with hypofractionated RT in a spontaneous canine oral melanoma model. Our rationale is that the nanoparticle immune adjuvants will combine with RT-induced ICD to expand the tumor specific effector T cell population resulting in longer local and distant tumor remission.

Dogs are genetically variable animals with a cancer incidence and prevalence, tumor type, and tissue origin site that is comparable to human cancer. Behaviorally, the canine oral melanoma is very similar to an aggressive human dermal melanoma.<sup>30</sup> Canine oral melanomas grow at rates roughly similar to aggressive human melanoma, metastasize aggressively, and are often well-established when detected in the oral cavity. Most oral canine melanomas are treated with excisional surgery with completeness of tumor removal status unknown at the time of surgery. Approximately 85–90% of these tumors recur locally and/or at distant site within 5–9 months. RT alone, using varied total dose and fraction delivery regimens, has demonstrated a similar prognosis, with a median recurrence/metastasis time of 5–7 months. Variables such as age, tumor size, and tumor location influence the prognosis;

however, most studies suggest that these influences do not alter the time to recurrence or metastasis more than 20% for any situation.<sup>30–33</sup>

## METHODS

**Canine Oral Melanoma Patient Recruitment and Experimental Treatment.** The canine oral melanoma cancer patients were recruited from local veterinary practices. Study inclusion required a tissue biopsy diagnosis of oral malignant melanoma, a tumor less than 5 cm in diameter, the lack of both metastatic disease (clinical examination/CT scan) and chronic-life threatening disease, and legally documented owner consent. All diagnostic examinations and clinical treatments were performed at Geisel School of Medicine, Dartmouth Hitchcock Medical Center, Lebanon, NH. Referring veterinarians remained part of the clinical team, receiving all relevant patient treatment and health information from the Dartmouth team. When appropriate, the referral veterinarians performed follow-up examinations and supportive treatments.

**Radiation Treatment Planning and Delivery.** Following generation of a CT-based 3-D radiation treatment plan, all patients received 6 doses of 6 Gy photon radiation (36 Gy total, Varian 2100C linear accelerator) to the local tumor and 1 cm peri-tumor margin. Treatment was applied on a Monday, Wednesday, Friday schedule over a 2 week period. All treatments were performed under general anesthesia.

**Magnetic Iron Oxide Nanoparticle (IONP) Hyperthermia Treatment (mNPH).** NT-01 iron oxide nanoparticles (Micromod Partikeltechnologie GmbH, Rostock, Germany) were used. NT-01 magnetic nanoparticles consist of multiple ~20 nm hematite crystals embedded in a dextran matrix core (40 nm diameter), surrounded by a dextran shell. The final average hydrodynamic NP diameter was 110 nm. The mNP were delivered in a sterile water-based NP concentration of 44 mg/mL with an iron concentration of 28 mg/mL and a volume of 500  $\mu$ L. The amount of iron oxide nanoparticles was constant regardless of tumor size. A cooled Fluxtrol pancake coil (20 cm diameter) or a cooled custom copper helical coil, with an inner diameter of 20 cm, was used to generate AMF. The AMF coils were powered by a variable 25 KW generator (Huttinger Elektronik GmbH, Freiburg, Germany) at a field of 150 kHz and 400 Oe. The AMF coil and generator were cooled by a chiller (Tek-Temp Instruments, Croydon, PA) operating at 20 °C and 4 gallons per minute. mNPs were delivered intratumorally at a dose of 7.5 mg into 4 equally spaced tumor sites. mNP were incubated for 90 min prior to AMF exposure. Tumors were treated to a thermal dose equivalent to 43 °C for 60 min (cumulative equivalent minutes/CEM = 60).<sup>34</sup> Each tumor receiving mNPH was treated twice (once each week) over the 2 week treatment period. Temperatures were measured using 0.3 mm fiberoptic sensors (FISO Corp, Quebec, Canada) accurate to 0.1 °C placed in 3 tumor sites, 2 peri-tumor sites, and 1 core/rectum site.

**Plant Virus-Like Nanoparticles (VLP).** VLPs from cowpea mosaic virus were produced in plants.<sup>27</sup> VLPs were delivered intratumorally 2 times/week  $\times$  2 weeks (four treatments). Each 200  $\mu$ g (200  $\mu$ L) intratumoral VLP injection was distributed in 3 locations within the tumor. The amount of VLPs per treatment was constant regardless of the tumor size.

**Treatments and End Points.** Using a feasibility study design, five tumors were treated with four treatment regimens:

Table 1. Data Summary from the Five Patients That Are the Subject of This Study

treatment	patient information	pretreatment cellularity	post-treatment cellularity	patient outcome
hypofractionated radiation	10 year old, male, Labrador	tumor 68% lymph/mono 12% PMN 2% stroma 19%	tumor 55% lymph/mono 15% PMN 4% stroma 26%	euthanized due to local and metastatic cancer; 5 months post treatment
magnetic nanoparticle hyperthermia	11 year old, male, Siberian Husky	tumor 70% lymph/mono 11% PMN 2% stroma 17%	tumor 26% lymph/mono 18% PMN 18% stroma 38%	euthanized due to local and metastatic cancer; 26 months post treatment
hypofractionated radiation + virus-like particles	7 year old male Labrador	tumor 74% lymph/mono 16% PMN 1% stroma 13%	tumor 18% lymph/mono 21% PMN 13% stroma 48%	tumor free when euthanized due to GI torsion; 5 months post treatment
hypofractionated radiation + virus-like particles	12 year old, female Beagle	tumor 87% lymph/mono 6% PMN 1% stroma 13%	tumor 29% lymph/mono 45% PMN 9% stroma 17%	alive and tumor free; 20 months post treatment
hypofractionated radiation + virus-like particles + magnetic nanoparticle hyperthermia	9 year old, male Rottweiler	tumor 69% lymph/mono 14% PMN 2% stroma 25%	tumor 21% lymph/mono 22% PMN 11% stroma 46%	tumor free when euthanized due to noncancer issue: 10 months post treatment

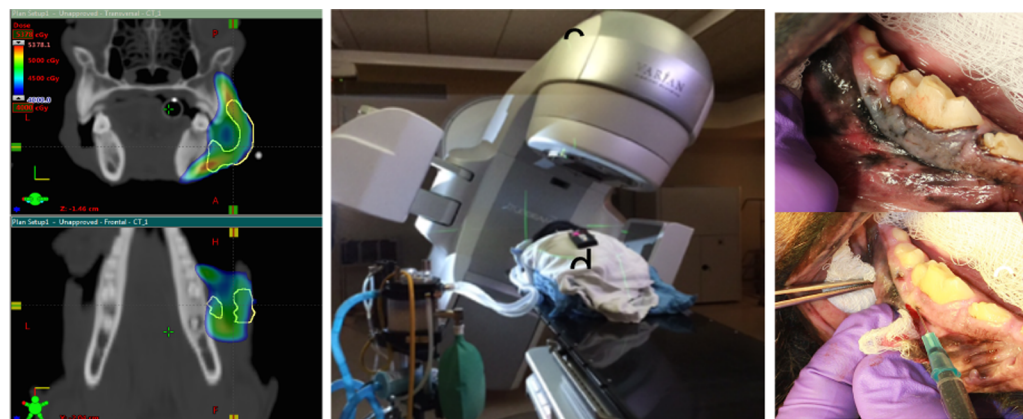


**Figure 1.** Treatment of 9 year old Rottweiler with left mandibular oral melanoma. The tumor received  $6 \times 6$  Gy radiation, mNPH, and  $4 \times 200 \mu\text{g}$  of VLP. Left figures demonstrate the 3-D radiation treatment plan. Center figure shows patient in position for radiation delivery via the Varian Truebeam linear accelerator. Right figures show intratumoral injection of VLP.

- Hypofractionated radiation therapy (HFRT) @  $36 \text{ Gy}$  ( $6 \times 6 \text{ Gy}$ ).  $n = 1$ ,
- Magnetic/iron oxide nanoparticle hyperthermia (mNPH) @  $2 \times \text{CEM } 60$ .  $n = 1$
- HFRT + virus-like nanoparticles (VLP) @  $4 \times 200 \mu\text{g}$ .  $n = 2$
- HFRT + VLP + mNPH.  $n = 1$

Clinical end points included time to recurrence or metastasis and survival. Primary tumor response and potential metastasis was assessed clinically every 2 weeks for 3 months post-treatment and every 2–3 months thereafter, including a radiological exam (X-ray, CT). The immunopathology end point was histomorphological quantification of the cell/tissue composition of the tumor. Samples were assessed before and 14–21 days post-treatment.

**Quantification of Tumor Cellularity Following RT, mNPH and/or VLP.** To assess the immune response, quantification of the inflammatory/immune cell infiltration into the tumor and the peri-tumoral region was performed in tissues taken before treatment and 14–21 days following treatment completion. We used the well-established Chalkley histomorphometric technique to quantitate cell types in standard histology images.<sup>35</sup> This method, using conventional hematoxylin and eosin (H&E) stained slides, consists of placing a 100-point optical grid over randomly determined microscopic fields (we used 10 fields). At each cross-hair grid point, the cell or tissue type is identified by its morphology and recorded, providing a relative cell/tissue composition of the sample being assessed. We assessed four different cell/tissue parameters: (a) tumor cell, (b) mononuclear immune cell (lymphocyte/

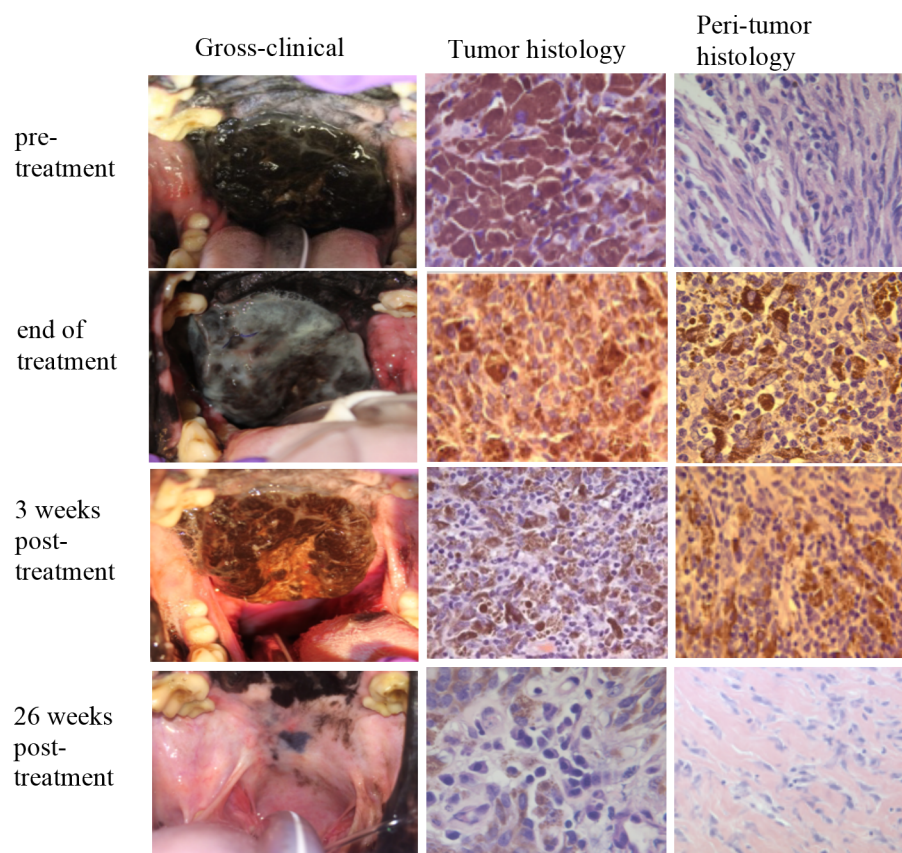


**Figure 2.** Tumor regression and cellular changes in a large soft palate oral melanoma following HFRT and VLP treatment. The images are from a 12-year old female beagle patient. In addition to complete tumor resolution, that is now durable at 20 months, there is a dramatic inflammatory/immune response in the weeks following treatment. The figure provides visual comparison of the gross clinical response, and the level of immune cell infiltration in the tumor and peri-tumor tissue at the selected times and illustrates sample histologic images used for quantitation of immune infiltrate in Table 1. The response is largely mononuclear cell (macrophage/lymphocyte, small blue cells with high nucleus/cytoplasm ratio); however, pockets of neutrophils are also seen in some areas. As noted in the final two histology photomicrographs, while there is no residual tumor, there is some ongoing active fibroplasia, however most of the response at this point is mature fibrosis.

monocyte/macrophage), (c) polymorphonuclear cells (PMN, neutrophils), and stroma (fibrous connective tissues, vascular tissue, etc.). Hematoxylin and eosin stain is a routine histochemical dye-type stain that is commonly used to assess morphological cell and tissue detail. H&E stain does not involve an antibody and is not capable of tagging/staining a specific molecule or protein. Rather, the eosin (pink color) is an acidic dye that stains almost all cellular proteins, and the hematoxylin (blue color) is basophilic dye that stains nucleic acid (nucleus/DNA).

## RESULTS

This study reports results from RT combined with nanotechnology-based in situ vaccination in canine oral melanoma. The application of radiation utilized clinical equipment and CT-based 3-D treatment planning similar to what is done for human patients. Study results, using quantitative tumor composition histomorphometry, demonstrate the effects of combining hypofractionated RT with mNPH and/or VLP (Figure 2, Table 1). Histomorphometric quantification of the cellular composition of the melanoma tumors<sup>35</sup> before and 14–21 days after treatment was used to document cellular immunopathology changes. Time to tumor recurrence and/or metastasis demonstrate clinical treatment responses. The radiation treatment utilized clinical treatment planning as shown in Figure 1, and radiation was applied using clinical

treatment equipment. This enabled the control and precision of radiation dosimetry that is utilized clinically.

Tumor response data from five patients is summarized in Table 1. It is important to note that while we quantified the immune cell response in the tumor and peri-tumor normal tissue in all patients, peri-tumor normal tissue samples (biopsies) were more challenging to acquire and were not acquired from all patients. Therefore, although we give an example of the comparative tumor and peri-tumor normal tissue response in the Figure 2 patient, the cell response quantification information demonstrated in Table 1 includes only pretreatment and post-treatment information for tumor tissues, not peri-tumor tissue.

Although the sample is small, the combination of HFRT+VLP appears to be the most promising treatment, since both patients fully resolved the treated tumor, neither patient relapsed, and one patient is clinically cancer free 20 months after treatment, which is well outside of the expected time to relapse of 5–9 months. The histology of multiple tumor and peri-tumor tissue samples at different time points from this patient is shown (Figure 2, 12 month old female beagle). This oral melanoma case received  $6 \times 6$  Gy HFRT (days 1, 3, 5, 7, 9, 12) and  $4 \times 200$   $\mu$ g VLP (days 2, 5, 7, 12) to treat an  $\sim 35$  cm<sup>3</sup> melanoma located on the dorsal soft palate that virtually occluded the oropharynx. While the complete clinical response of this very large melanoma is striking, the immunological

reaction in the tumor and peri-tumor tissue is noteworthy for correlating with the clinical response. It is especially relevant to note the dramatic increase in immune cell infiltration on the final day of treatment in the peri-tumor and 3 weeks post-treatment, in both the tumor and peri-tumor tissue. While there is a complete array of immune cell types in this response, the increase in lymphocytes/monocyte is notable.

## DISCUSSION

In this feasibility, immunopathology, and efficacy study of the treatment of spontaneous canine oral melanoma tumors using HFRT and nanotechnology-based immunotherapy, we demonstrate a significant increase in immune cell infiltration of tumors receiving HFRT with the nanotechnology immune adjuvants, especially the VLP adjuvants. However, the low numbers of patients per treatment arm precludes statistical analysis. The study successfully demonstrates the feasibility, safety, and promising efficacy of these treatments in a highly translatable spontaneous preclinical model.

Specifically, the data enables assessment of changes in cellularity between the pretreatment biopsy and the post-treatment biopsy 14–21 days after treatment completion. There appears to be a preliminary correlation between increased leukocyte concentration in the tumor, (potentially turning an immunologically “cold” tumor into a “hot” tumor), and clinical efficacy. The “RT only” patient had very minimal changes in leukocyte concentration and was the only patient that had metastatic disease at 5 months post-treatment, within the expected time to metastasis of less than 9 months. Treatments that included VLP and/or mNPH all had very clear increases of leukocyte numbers in the tumor due to treatment. The increased leukocyte numbers were accompanied by improvement over the expected outcome with two animals being euthanized tumor free for unrelated clinical reasons 5 months (HFRT + VLP) and 10 months (HFRT + mNPH + VLP) post-treatment, and one dog (HFRT + VLP, Figure 2) who remains tumor free 20 months after treatment.

The histomorphometric technique used to identify and quantify the immune cell response in the treated tumors is a standard pathological approach requiring histomorphological skills. This approach is very reproducible and accurate for determination of global cellular immune responses in the treated tumor/normal tissue. However, the information it provides is limited from a specific immune cell identification standpoint, and specific immunohistochemical (IHC) labeling will be necessary to define the specific types of cells involved in the immune infiltrate. While appropriate immune cell IHC antibodies are available for many standard immune cell markers in dogs, labeling inconsistencies associated with individual dogs and markers precluded effective use in this study. It should also be noted that the hypofractionated radiation treatment regimen (6 × 6 Gy over 2 weeks) is not a global clinical standard but is becoming so in a variety of cancer sites, including breast cancer.

## AUTHOR INFORMATION

### Corresponding Authors

\*E-mail: (N.F.S.) [nicole.steinmetz@case.edu](mailto:nicole.steinmetz@case.edu)

\*E-mail: (S.N.F.) [fiering@dartmouth.edu](mailto:fiering@dartmouth.edu)

### ORCID

Steven N. Fiering: [0000-0003-0624-974X](https://orcid.org/0000-0003-0624-974X)

### Notes

The authors declare no competing financial interest.

## ACKNOWLEDGMENTS

This work was funded in part by NIH NCI U01CA218292 to N.F.S. and S.N.F.; Munck-Pfefferkorn grant from the Geisel School of Medicine at Dartmouth to P.J.H. and S.N.F.; NIH U54 CA151662 grant to P.J.H. and S.N.F.

## REFERENCES

- (1) Hiniker, S. M.; Chen, D. S.; Reddy, S.; Chang, D. T.; Jones, J. C.; Mollick, J. A.; Swetter, S. M.; Knox, S. J. A systemic complete response of metastatic melanoma to local radiation and immunotherapy. *Transl Oncol* **2012**, *5* (6), 404–7.
- (2) Grass, G. D.; Krishna, N.; Kim, S. The immune mechanisms of abscopal effect in radiation therapy. *Curr. Probl Cancer* **2016**, *40* (1), 10–24.
- (3) Melero, I.; Berman, D. M.; Aznar, M. A.; Korman, A. J.; Pérez Gracia, J. L.; Haanen, J. Evolving synergistic combinations of targeted immunotherapies to combat cancer. *Nat. Rev. Cancer* **2015**, *15* (8), 457–472.
- (4) Toraya-Brown, S.; Sheen, M. R.; Zhang, P.; Chen, L.; Baird, J. R.; Demidenko, E.; Turk, M. J.; Hoopes, P. J.; Conejo-Garcia, J. R.; Fiering, S. Local hyperthermia treatment of tumors induces CD8(+) T cell-mediated resistance against distal and secondary tumors. *Nano-medicine* **2014**, *10* (6), 1273–85.
- (5) Stone, H. B.; Peters, L. J.; Milas, L. Effect of host immune capability on radiocurability and subsequent transplantability of a murine fibrosarcoma. *J. Natl. Cancer Inst* **1979**, *63* (5), 1229–1235.
- (6) Fridman, W. H.; Pages, F.; Sautès-Fridman, C.; Galon, J. The immune contexture in human tumours: impact on clinical outcome. *Nat. Rev. Cancer* **2012**, *12* (4), 298–306.
- (7) Twyman-Saint Victor, C.; Rech, A. J.; Maity, A.; Rengan, R.; Pauken, K. E.; Stelekati, E.; Benci, J. L.; Xu, B.; Dada, H.; Odorizzi, P. M.; Herati, R. S.; Mansfield, K. D.; Patsch, D.; Amaravadi, R. K.; Schuchter, L. M.; Ishwaran, H.; Mick, R.; Pryma, D. A.; Xu, X.; Feldman, M. D.; Gangadhar, T. C.; Hahn, S. M.; Wherry, E. J.; Vonderheide, R. H.; Minn, A. J. Radiation and dual checkpoint blockade activate non-redundant immune mechanisms in cancer. *Nature* **2015**, *520* (7547), 373–7.
- (8) Deng, L.; Liang, H.; Burnette, B.; Beckett, M.; Darga, T.; Weichselbaum, R. R.; Fu, Y. X. Irradiation and anti-PD-L1 treatment synergistically promote antitumor immunity in mice. *J. Clin. Invest.* **2014**, *124* (2), 687–95.
- (9) Cho, Y.; Chang, J. S.; Rha, K. H.; Hong, S. J.; Choi, Y. D.; Ham, W. S.; Kim, J. W.; Cho, J. Does Radiotherapy for the Primary Tumor Benefit Prostate Cancer Patients with Distant Metastasis at Initial Diagnosis? *PLoS One* **2016**, *11* (1), e0147191.
- (10) Tsai, M. H.; Cook, J. A.; Chandramouli, G. V.; DeGraff, W.; Yan, H.; Zhao, S.; Coleman, C. N.; Mitchell, J. B.; Chuang, E. Y. Gene expression profiling of breast, prostate, and glioma cells following single versus fractionated doses of radiation. *Cancer Res.* **2007**, *67* (8), 3845–52.
- (11) John-Aryankalayil, M.; Palayoor, S. T.; Cerna, D.; Simone, C. B., 2nd; Falduto, M. T.; Magnuson, S. R.; Coleman, C. N. Fractionated radiation therapy can induce a molecular profile for therapeutic targeting. *Radiat. Res.* **2010**, *174* (4), 446–58.
- (12) Dewan, M. Z.; Galloway, A. E.; Kawashima, N.; Dewyngaert, J. K.; Babb, J. S.; Formenti, S. C.; Demaria, S. Fractionated but not single-dose radiotherapy induces an immune-mediated abscopal effect when combined with anti-CTLA-4 antibody. *Clin. Cancer Res.* **2009**, *15* (17), 5379–88.
- (13) Postow, M.; Callahan, M. K.; Wolchok, J. D. Beyond cancer vaccines: a reason for future optimism with immunomodulatory therapy. *Cancer J.* **2011**, *17* (5), 372–8.
- (14) Starnell, E. F.; Wolchok, J. D.; Gnjatic, S.; Lee, N. Y.; Brownell, I. The abscopal effect associated with a systemic anti-melanoma immune response. *Int. J. Radiat. Oncol., Biol., Phys.* **2013**, *85* (2), 293–5.

- (15) Demaria, S.; Formenti, S. C. Radiation as an immunological adjuvant: current evidence on dose and fractionation. *Front. Oncol.* **2012**, *2*, 153.
- (16) Barker, C. A.; Postow, M. A. Combinations of radiation therapy and immunotherapy for melanoma: a review of clinical outcomes. *Int. J. Radiat. Oncol., Biol., Phys.* **2014**, *88* (5), 986–97.
- (17) Siva, S.; MacManus, M. P.; Martin, R. F.; Martin, O. A. Abscopal effects of radiation therapy: a clinical review for the radiobiologist. *Cancer Lett.* **2015**, *356* (1), 82–90.
- (18) Crittenden, M. R.; Savage, T.; Cottam, B.; Baird, J.; Rodriguez, P. C.; Newell, P.; Young, K.; Jackson, A. M.; Gough, M. J. Expression of arginase I in myeloid cells limits control of residual disease after radiation therapy of tumors in mice. *Radiat. Res.* **2014**, *182* (2), 182–90.
- (19) Golden, E. B.; Apetoh, L. Radiotherapy and immunogenic cell death. *Semin Radiat Oncol* **2015**, *25* (1), 11–7.
- (20) Lee, Y.; Auh, S. L.; Wang, Y.; Burnette, B.; Wang, Y.; Meng, Y.; Beckett, M.; Sharma, R.; Chin, R.; Tu, T.; Weichselbaum, R. R.; Fu, Y. X. Therapeutic effects of ablative radiation on local tumor require CD8+ T cells: changing strategies for cancer treatment. *Blood* **2009**, *114* (3), 589–95.
- (21) Apetoh, L.; Ghiringhelli, F.; Tesniere, A.; Obeid, M.; Ortiz, C.; Criollo, A.; Mignot, G.; Maiuri, M. C.; Ullrich, E.; Saulnier, P.; Yang, H.; Amigorena, S.; Ryffel, B.; Barrat, F. J.; Saftig, P.; Levi, F.; Lidereau, R.; Nogues, C.; Mira, J. P.; Chompret, A.; Joulin, V.; Clavel-Chapelon, F.; Bourhis, J.; Andre, F.; Delaloge, S.; Tursz, T.; Kroemer, G.; Zitvogel, L. Toll-like receptor 4-dependent contribution of the immune system to anticancer chemotherapy and radiotherapy. *Nat. Med.* **2007**, *13* (9), 1050–9.
- (22) Jordan, A.; Scholz, R.; Maier-Hauff, K.; van Landeghem, F. K.; Waldoefner, N.; Teichgraeber, U.; Pinkernelle, J.; Bruhn, H.; Neumann, F.; Thiesen, B.; von Deimling, A.; Felix, R. The effect of thermotherapy using magnetic nanoparticles on rat malignant glioma. *J. Neuro-Oncol.* **2006**, *78* (1), 7–14.
- (23) Maier-Hauff, K.; Rothe, R.; Scholz, R.; Gneveckow, U.; Wust, P.; Thiesen, B.; Feussner, A.; von Deimling, A.; Waldoefner, N.; Felix, R.; Jordan, A. Intracranial thermotherapy using magnetic nanoparticles combined with external beam radiotherapy: results of a feasibility study on patients with glioblastoma multiforme. *J. Neuro-Oncol.* **2007**, *81* (1), 53–60.
- (24) Johannsen, M.; Gneveckow, U.; Taymoorian, K.; Thiesen, B.; Waldoefner, N.; Scholz, R.; Jung, K.; Jordan, A.; Wust, P.; Loening, S. A. Morbidity and quality of life during thermotherapy using magnetic nanoparticles in locally recurrent prostate cancer: results of a prospective phase I trial. *Int. J. Hyperthermia* **2007**, *23* (3), 315–23.
- (25) Zhang, G.; Liao, Y.; Baker, I. Surface Engineering of Core/Shell Iron/Iron Oxide Nanoparticles from Microemulsions for Hyperthermia. *Mater. Sci. Eng., C* **2010**, *30* (1), 92–97.
- (26) Toraya-Brown, S.; Fiering, S. Local tumour hyperthermia as immunotherapy for metastatic cancer. *Int. J. Hyperthermia* **2014**, *30* (8), 531–9.
- (27) Lizotte, P. H.; Wen, A. M.; Sheen, M. R.; Fields, J.; Rojanasopondist, P.; Steinmetz, N. F.; Fiering, S. In situ vaccination with cowpea mosaic virus nanoparticles suppresses metastatic cancer. *Nat. Nanotechnol.* **2016**, *11* (3), 295–303.
- (28) Lee, K. L.; Murray, A. A.; Le, D. H. T.; Sheen, M. R.; Shukla, S.; Commandeur, U.; Fiering, S.; Steinmetz, N. F. Combination of Plant Virus Nanoparticle-Based in Situ Vaccination with Chemotherapy Potentiates Antitumor Response. *Nano Lett.* **2017**, *17* (7), 4019–4028.
- (29) Giustini, A. J.; Petryk, A. A.; Cassim, S. M.; Tate, J. A.; Baker, I.; Hoopes, P. J. Magnetic Nanoparticle Hyperthermia in Cancer Treatment. *Nano LIFE* **2010**, *01*, 17.
- (30) Bergman, P. J. Canine oral melanoma. *Clin Tech Small Anim Pract* **2007**, *22* (2), 55–60.
- (31) Gardner, H. L.; Fenger, J. M.; London, C. A. Dogs as a Model for Cancer. *Annu. Rev. Anim. Biosci.* **2016**, *4*, 199–222.
- (32) Williams, L. E.; Packer, R. A. Association between lymph node size and metastasis in dogs with oral malignant melanoma: 100 cases (1987–2001). *J. Am. Vet. Med. Assoc.* **2003**, *222* (9), 1234–6.
- (33) Proulx, D. R.; Ruslander, D. M.; Dodge, R. K.; Hauck, M. L.; Williams, L. E.; Horn, B.; Price, G. S.; Thrall, D. E. A retrospective analysis of 140 dogs with oral melanoma treated with external beam radiation. *Vet Radiol Ultrasound* **2003**, *44* (3), 352–359.
- (34) Sapareto, S. A.; Dewey, W. C. Thermal dose determination in cancer therapy. *Int. J. Radiat. Oncol., Biol., Phys.* **1984**, *10* (6), 787–800.
- (35) Chalkley, H. W. Method for the quantitative morphometric analysis of tissues. *J. Natl. Cancer Inst.* **1943**, *4*, 47–53.